



JOURNAL OF  
APPLIED  
CRYSTALLOGRAPHY

**Volume 56 (2023)**

**Supporting information for article:**

**AlphaFold predicted protein structures and small-angle X-ray scattering: insights from an extended examination of selected data in the Small-Angle Scattering Database**

**Emre Brookes, Mattia Rocco, Patrice Vachette and Jill Trehwella**

## S1. CRY SOL 3.2 Calculations

As noted in the main text, a recent CRY SOL release (version 3.2) has an option to use a different hydration scheme with dummy water beads, which in principle should be more efficient in dealing with structures presenting extended non-structured segments (Franke *et al.*, 2017). Since completing the original study, CRY SOL 3.2 has been made accessible from within US-SOMO and will be made available to the general user in the next planned release. To evaluate the potential impact of the alternate hydration scheme, we repeated all the NNLS fits using  $I(q)$  profiles generated using CRY SOL 3.2 with the dummy water option.

For SASDBP9 (**Table S2**), the NNLS fit with CRY SOL 3.2-generated  $I(q)$  profiles yielded the same three highest contributing structures as was obtained with CRY SOL 2.8, in two cases with comparable percentages, with some differences in the minor population structures and a slightly improved  $\chi^2$  value. The subsequent WAXSiS-based NNLS fit yielded the same results as that based on the CRY SOL 2.8-produced data. When all structures based on both  $P(r)$  and both CRY SOL versions NNLS fits were included, again the NNLS returned identical results as those that included only the CRY SOL 2.8-based selected structures. Thus, in this case it appears that utilizing CRY SOL 3.2 did not provide a different pre-selection of contributing structures over CRY SOL 2.8.

The NNLS fits for SASDF83 (**Table S3**) using CRY SOL 3.2-generated  $I(q)$  profiles selected the same three structures contributing significantly (>10%) as for CRY SOL 2.8, but with different percentages, and, as for the AF-Q16543/SASDBP9 set, with a slightly worse  $\chi^2$  value. In this case, the subsequent WAXSiS-based NNLS selected four out of six structures in common with those selected by the WAXSiS NNLS fit including the CRY SOL 2.8 pre-selected models, with variable percentages and practically identical  $\chi^2$ . The very same result was obtained when the NNLS fit was performed with WAXSiS calculated  $I(q)$  profiles from structure sets selected using all methods.

The NNLS fits with the CRY SOL 3.2-generated  $I(q)$  profiles for SASDM77 (**Table S4**) selected twelve structures, five of which were in common with the ten structures selected in the CRY SOL 2.8-NNLS fit, albeit with different percentages, and again a slightly worse  $\chi^2$  value. The subsequent WAXSiS-based NNLS fit produced results close to those based on the CRY SOL 2.8 selections, in many cases with similar percentages, and with a practically identical  $\chi^2$  value. In this case, when all selected structures based on both  $P(r)$  and both CRY SOL versions NNLS fits were included, the NNLS returned mixed results, and with an identical  $\chi^2$  value as the other two. As in the previous two cases, using CRY SOL 3.2 over 2.8 provided no clear distinction when all models pre-selected were then analyzed based on WAXSiS computations. If anything, the CRY SOL 3.2-based NNLS fit selected two structures with a very large  $d_{\max}$  (275 and 281 Å), one of which was confirmed at a significant level (structure 12,700 in **Table S4**, ~10%) by the subsequent WAXSiS-based NNLS fits.

**Table S1** MMC runs summary.

| AF Accession code                   | Q16543             | Q06817  | Q9UK19          |
|-------------------------------------|--------------------|---------|-----------------|
| SASBDB Accession code               | SASDBP9            | SASDF83 | SASDM77         |
| Residue ranges for flexible regions | 121-139<br>343-378 | 170-210 | 1-54<br>273-336 |
| Number of trial attempts            | 20,000             | 20,000  | 20,000          |
| Accepted structures                 | 15,661             | 14,582  | 17,284          |
| Sub-selection stride                | 9                  | 15      | 10              |
| Sub-selected structures             | 1,740              | 972     | 1,728           |
| AF starting structure $R_g$ (Å)     | 50.0               | 30.5    | 41.4            |
| Lowest $R_g$ (Å)                    | 30.5               | 24.1    | 29.0            |
| Highest $R_g$ (Å)                   | 56.1               | 73.3    | 93.8            |
| Average accepted $R_g$ (Å)          | 46.5               | 49.9    | 63.3            |

**Table S2** Models selected by NNLS from the data produced by the various methods, including CRY SOL 3.2 with dummy waters, and their percentages, for the SASDBP9/AF-Q16543 system. The WAXSiS-based NNLS fits included the two  $P(r)$  datasets and either one of the CRY SOL version-based dataset (e.g., "w CR 2.8") or both CRY SOL versions-based datasets ("all").

| Model #  | $P(r)$<br>no err wt | $P(r)$<br>err wt | CRY SOL<br>2.8 | CRY SOL<br>3.2 | WAXSiS<br>w CR 2.8 | WAXSiS<br>w CR 3.2 | WAXSiS<br>all |
|----------|---------------------|------------------|----------------|----------------|--------------------|--------------------|---------------|
| 0        |                     |                  |                |                | 4.5                | 4.5                | 4.5           |
| 90       |                     |                  |                |                |                    |                    |               |
| 459      |                     |                  | 44.3           | 38.4           | 25.8               | 25.8               | 25.8          |
| 1404     |                     |                  |                | 1.0            |                    |                    |               |
| 1494     |                     | 4.4              | 0.4            | 6.2            |                    |                    |               |
| 1503     |                     | 2.4              |                |                |                    |                    |               |
| 2610     | 41.3                | 61.6             | 24.6           | 32.3           | 26.3               | 26.3               | 26.3          |
| 4617     |                     |                  | 0.6            | 1.7            |                    |                    |               |
| 5166     |                     | 2.6              |                |                |                    |                    |               |
| 6543     |                     | 12.7             |                |                |                    |                    |               |
| 7263     |                     |                  |                | 0.1            |                    |                    |               |
| 7371     | 1.5                 |                  |                |                |                    |                    |               |
| 7929     | 14.3                |                  |                |                |                    |                    |               |
| 7938     |                     |                  | 0.2            | 2.3            | 6.1                | 6.1                | 6.1           |
| 8208     |                     |                  |                | 0.6            |                    |                    |               |
| 9009     | 0.6                 |                  |                |                |                    |                    |               |
| 9387     | 1.7                 |                  |                |                |                    |                    |               |
| 9558     | 16.3                | 8.3              |                |                | 13.0               | 13.0               | 13.0          |
| 9783     |                     |                  |                | 0.9            |                    |                    |               |
| 9801     | 2.3                 |                  |                |                | 6.1                | 6.1                | 6.1           |
| 9819     | 2.7                 |                  |                |                |                    |                    |               |
| 9855     | 8.9                 |                  |                |                |                    |                    |               |
| 10323    | 2.5                 |                  |                |                |                    |                    |               |
| 11169    |                     |                  |                | 11.0           |                    |                    |               |
| 11880    |                     |                  | 7.3            |                |                    |                    |               |
| 11943    | 8.0                 |                  |                |                | 6.7                | 6.7                | 6.7           |
| 12393    |                     |                  | 22.5           | 5.6            | 11.4               | 11.4               | 11.4          |
| 15237    |                     | 8.0              |                |                |                    |                    |               |
| Sum %    | 100.0               | 100.0            | 100.0          | 100.0          | 100.0              | 100.0              | 100.0         |
| $\chi^2$ | 1.399               | 2.065            | 1.602          | 1.521          | 1.228              | 1.228              | 1.228         |

**Table S3** Models selected by NNLS from the data produced by the various methods, including CRY SOL 3.2 with dummy waters, and their percentages, for the SASDF83/AF-Q06187 system. The WAXSiS-based NNLS fits included the two  $P(r)$  datasets and either one of the CRY SOL version-based dataset (e.g., "w CR 2.8") or both CRY SOL versions-based datasets ("all").

| Model #  | $P(r)$<br>no err wt | $P(r)$<br>err wt | CRY SOL<br>2.8 | CRY SOL<br>3.2 | WAXSiS<br>w CR 2.8 | WAXSiS<br>w CR 3.2 | WAXSiS<br>all |
|----------|---------------------|------------------|----------------|----------------|--------------------|--------------------|---------------|
| 0        |                     |                  |                |                |                    |                    |               |
| 945      |                     |                  |                |                |                    |                    |               |
| 1350     |                     | 17.8             |                |                |                    |                    |               |
| 1440     |                     |                  | 2.2            |                |                    |                    |               |
| 1770     | 0.2                 | 5.0              |                |                |                    |                    |               |
| 1785     |                     | 10.1             |                |                |                    |                    |               |
| 2595     | 2.0                 |                  | 24.1           | 37.6           | 46.0               | 42.8               | 42.8          |
| 3150     |                     |                  |                | 0.4            |                    |                    |               |
| 3360     | 13.5                |                  |                |                |                    |                    |               |
| 3600     |                     |                  | 10.1           | 39.0           | 34.8               | 23.2               | 23.2          |
| 4500     |                     |                  | 23.1           |                |                    |                    |               |
| 6465     | 0.5                 | 9.3              |                |                |                    |                    |               |
| 7665     |                     | 1.7              |                |                | 5.7                | 2.7                | 2.7           |
| 7680     |                     | 6.7              |                |                |                    |                    |               |
| 7725     | 5.2                 |                  |                |                | 5.4                |                    |               |
| 7830     |                     |                  |                |                |                    |                    |               |
| 11850    |                     |                  | 8.2            |                |                    |                    |               |
| 11925    |                     |                  |                | 2.8            |                    | 9.3                | 9.3           |
| 11940    |                     |                  |                | 10.7           |                    |                    |               |
| 12180    | 1.2                 |                  |                |                |                    |                    |               |
| 12465    |                     | 4.2              |                |                |                    |                    |               |
| 12510    | 10.4                |                  |                |                |                    |                    |               |
| 12810    | 31.3                |                  |                |                | 2.5                | 14.4               | 14.4          |
| 12870    | 24.0                | 45.2             |                |                |                    |                    |               |
| 13245    | 11.7                |                  | 1.6            |                | 5.6                | 7.7                | 7.7           |
| 13845    |                     |                  | 30.7           | 9.5            |                    |                    |               |
| Sum %    | 100.0               | 100.0            | 100.0          | 100.0          | 100.0              | 100.0              | 100.0         |
| $\chi^2$ | 1.997               | 2.716            | 1.673          | 1.695          | 1.763              | 1.762              | 1.762         |

**Table S4** Models selected by NNLS from the data produced by the various methods, including CRY SOL 3.2 with dummy waters, and their percentages, for the SASDM77/AF-Q9UKA9 system. The WAXSiS-based NNLS fits included the two  $P(r)$  datasets and either one of the CRY SOL version-based dataset (e.g., "w CR 2.8") or both CRY SOL versions-based datasets ("all").

| Model #  | $P(r)$<br>no err wt | $P(r)$<br>err wt | CRY SOL<br>2.8 | CRY SOL<br>3.2 | WAXSiS<br>w CR 2.8 | WAXSiS<br>w CR 3.2 | WAXSiS<br>all |
|----------|---------------------|------------------|----------------|----------------|--------------------|--------------------|---------------|
| 0        |                     |                  |                |                |                    |                    |               |
| 20       |                     |                  | 14.2           | 23.9           | 14.1               | 10.3               | 13.3          |
| 460      |                     |                  | 19.4           |                |                    |                    |               |
| 2020     | 37.8                | 23.0             |                |                |                    |                    |               |
| 2030     |                     |                  |                | 7.1            |                    |                    |               |
| 2610     |                     | 8.3              |                |                |                    |                    |               |
| 3330     |                     |                  |                |                |                    |                    |               |
| 3430     |                     | 6.7              |                |                | 2.0                | 2.9                | 3.5           |
| 6680     | 19.3                | 23.0             | 24.3           | 18.0           | 23.9               | 21.8               | 24.3          |
| 7190     |                     |                  |                | 0.4            |                    |                    |               |
| 7290     |                     |                  | 1.3            |                |                    |                    |               |
| 7320     |                     |                  | 0.4            |                | 2.3                |                    | 1.7           |
| 7560     | 0.5                 |                  |                |                | 2.2                |                    |               |
| 8150     | 3.7                 |                  |                |                |                    | 9.8                |               |
| 8550     | 0.1                 |                  |                |                |                    |                    |               |
| 8560     | 1.0                 |                  |                | 7.8            | 7.8                | 1.2                | 2.0           |
| 8570     |                     |                  |                | 1.5            |                    |                    |               |
| 10330    |                     | 10.4             |                |                |                    |                    |               |
| 10900    |                     |                  | 7.9            | 12.8           | 5.0                |                    |               |
| 11920    | 13.0                |                  |                |                |                    |                    |               |
| 12140    |                     |                  |                | 1.5            |                    |                    |               |
| 12300    | 1.0                 | 20.1             | 2.8            |                |                    |                    |               |
| 12570    | 3.3                 |                  |                |                |                    |                    |               |
| 12700    |                     |                  |                | 0.5            |                    | 11.1               | 10.9          |
| 13440    | 2.6                 |                  |                |                |                    |                    |               |
| 14320    | 0.9                 |                  |                |                | 1.6                | 5.5                | 5.1           |
| 15210    | 16.6                |                  |                |                |                    |                    |               |
| 15240    |                     |                  |                | 0.2            |                    |                    |               |
| 15250    | 0.2                 | 8.5              | 22.1           | 13.2           | 32.5               | 29.4               | 32.3          |
| 16620    |                     |                  | 1.2            | 13.2           | 8.5                | 7.9                | 6.7           |
| 16930    |                     |                  | 6.4            |                |                    |                    | 0.3           |
| Sum %    | 100.0               | 100.0            | 100.0          | 100.0          | 100.0              | 100.0              | 100.0         |
| $\chi^2$ | 1.279               | 1.493            | 1.208          | 1.240          | 1.179              | 1.176              | 1.176         |

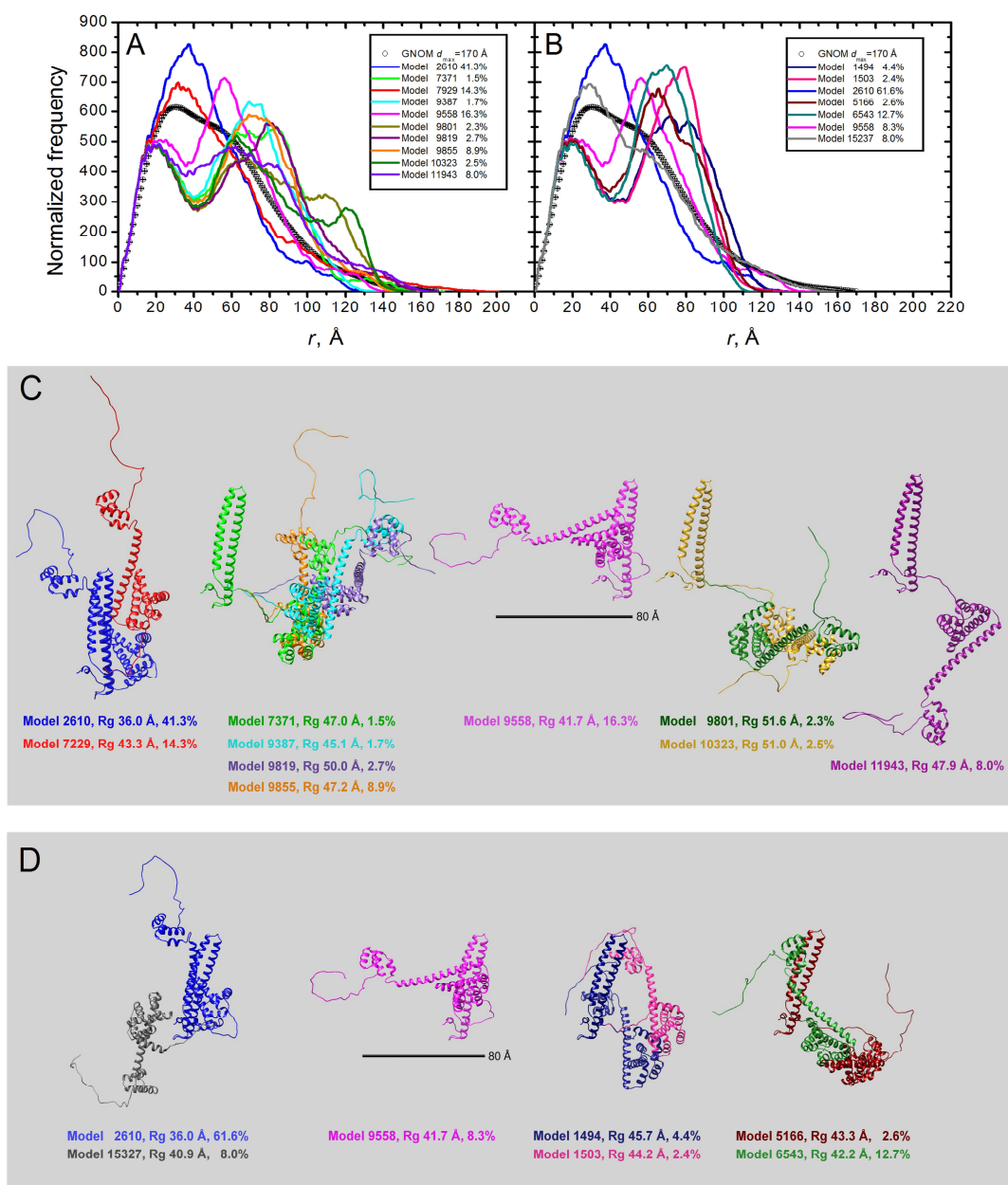


**Figure S1** A,B  $P(r)$  of the individual MMC-generated Q16543 models selected by NNLS without (A) and with (B) error weighting, with their percent contribution (various colours, see inside panels), overlaid to the experimentally-derived  $P(r)$  for SASDBP9. Model numbering is that of the original MMC pool. C,D Ribbon representations of the models selected by NNLS without (C) or with (D) error weighting. The models were all superposed using the N-terminal 25-110 sequence, and they were grouped into 5 (C) or 4 (D) classes according to a rough estimation of their respective  $P(r)$  shapes as plotted in A and B. Together with their percent contribution, the  $R_g$  of each model is also reported.

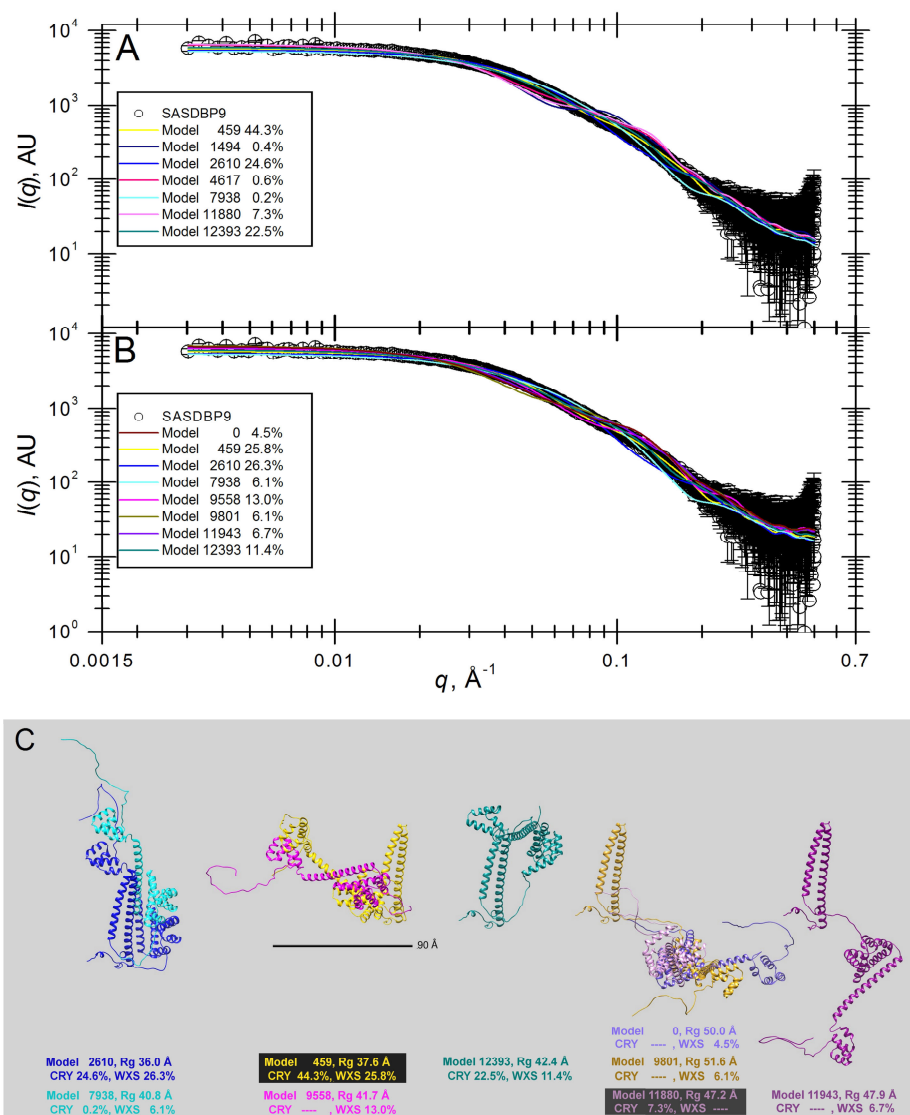


**Figure S2** **A,B**  $I(q)$  of the individual MMC-generated Q16543 models selected by NNLS from the CRYSOLOG 2.8-produced set (**A**), and from the WAXSiS-produced set comprising only the models selected by both the two  $P(r)$  and the  $I(q)$  CRYSOLOG 2.8 NNLS fits (**B**), with their percent contribution (various colours, see inside panels), superposed to the SASDBP9 experimental data. Model numbering is that of the original MMC pool. **C** Ribbon representations of the models selected by NNLS in panels **A** and **B**. The models were all superposed using the N-terminal 25-110 sequence, and they were grouped using the  $P(r)$ -derived clustering (**Figure S1C**) into four classes with one additional class (model 12393). Together with their percent contribution in each NNLS fit (CRY, CRYSOLOG; WXS, WAXSiS), the  $R_g$  of each model is also reported.



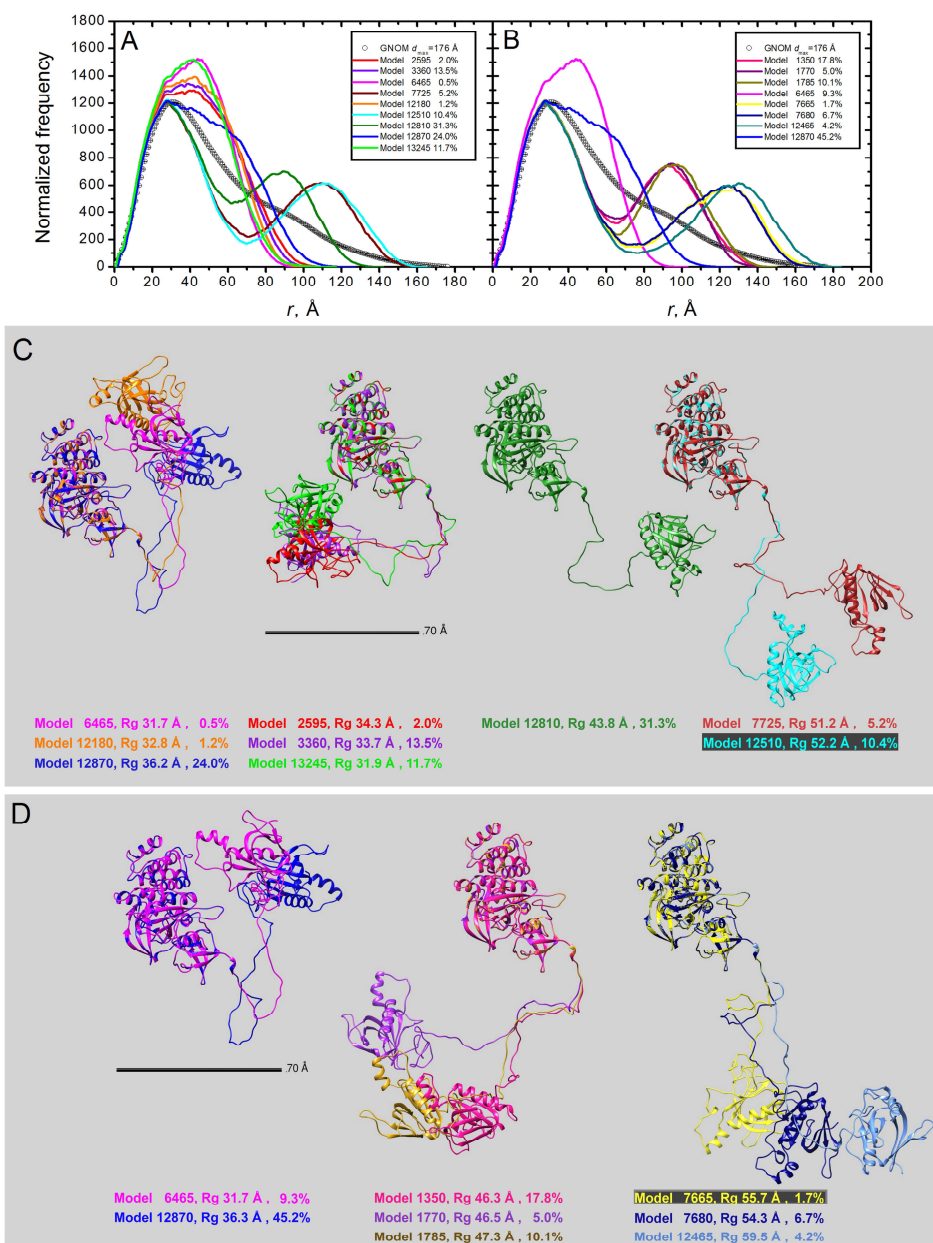


**Figure S3** A,B  $P(r)$  of the individual MMC-generated Q06187 models selected by NNLS without (A) and with (B) error weighting, with their percent contribution (various colours, see inside panels), overlaid to the experimentally-derived  $P(r)$  for SASDF83. Model numbering is that of the original MMC pool. C,D Ribbon representations of the models selected by NNLS without (C) or with (D) error weighting. The models were all superposed using the C-terminal 218-659 sequence, and they were grouped into four (C) or three (D) classes according to a rough estimation of their respective  $P(r)$  shapes as plotted in A and B, with an additional separation based on the spatial location of the N-terminal domain (left two classes in panel C). Together with their percent contribution, the  $R_g$  of each model is also reported.

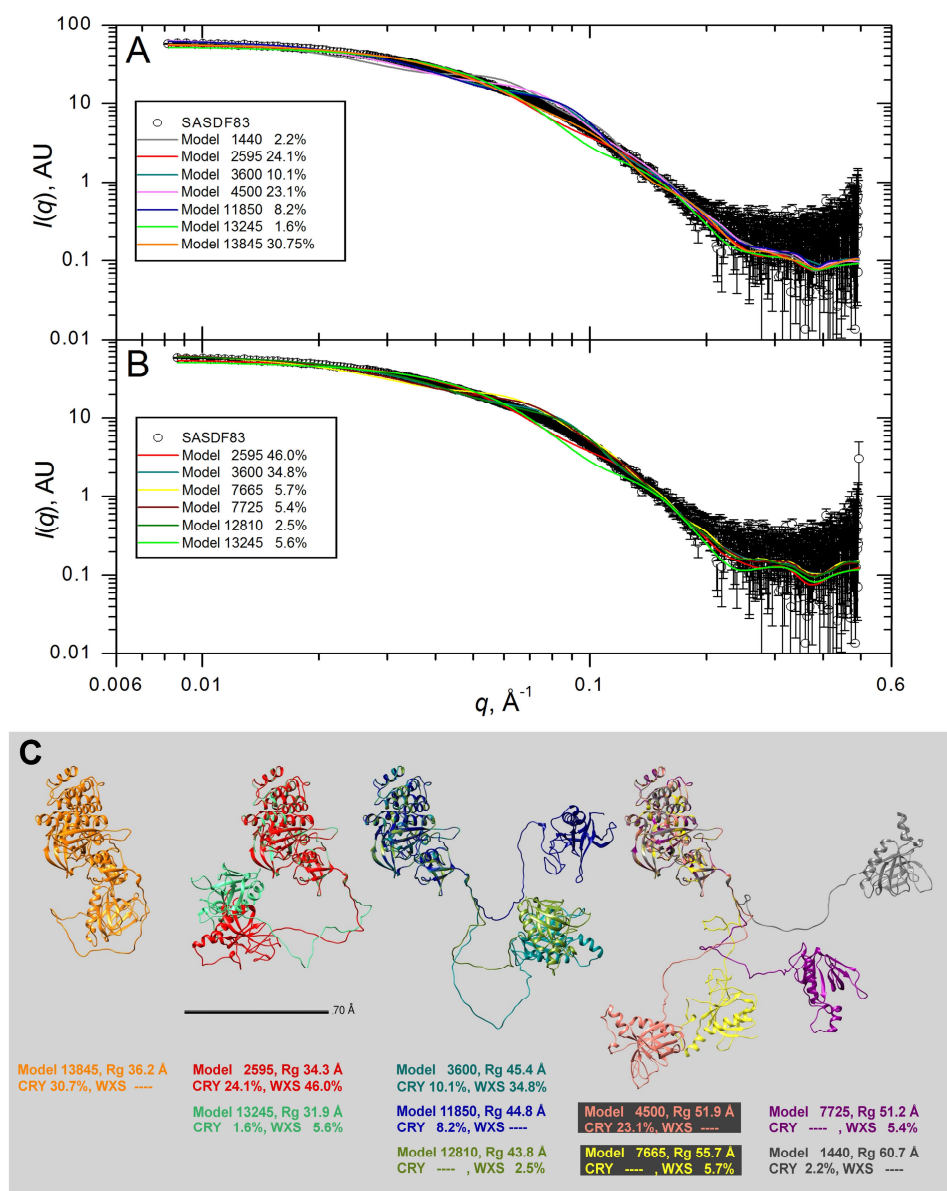


**Figure S4** **A,B**  $I(q)$  vs.  $q$  of the individual MMC-generated Q06187 models selected by NNLS from the CRYSOLO 2.8-produced set (**A**), and from the WAXSiS-produced set comprising only the models selected by both the two  $P(r)$  and the  $I(q)$  CRYSOLO 2.8 NNLS fits (**B**), with their percent contribution (various colours, see inside panels), superposed to the SASDF83 experimental data. Model numbering is that of the original MMC pool. **C,D** Ribbon representations of the models selected by NNLS in panels **A** and **B**, respectively. The models were all superposed using the C-terminal 218-659 sequence, and they were grouped using the  $P(r)$ -derived clustering of **Figure S3C**, with the replacement of the leftmost class with a single model. Together with their percent contribution in each NNLS fit (CRY, CRYSOLO; WXS, WAXSiS), the  $R_g$  of each model is also reported.

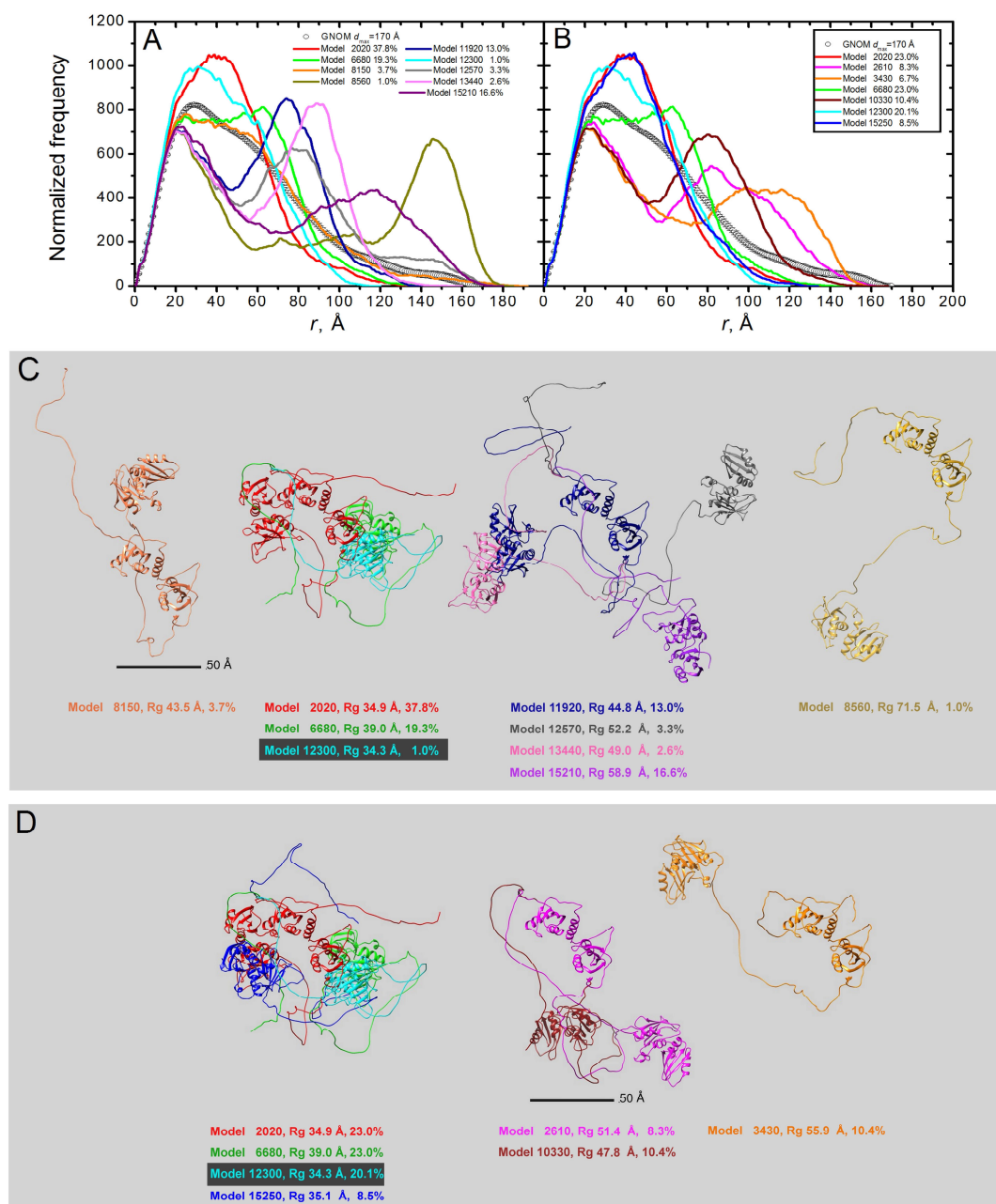


**Figure S5** **A,B**  $P(r)$  of the individual MMC-generated Q9UKA9 models selected by NNLS without (**A**) and with (**B**) error weighting, with their percent contribution (various colours, see inside panels), overlaid to the experimentally-derived  $P(r)$  for SASDM77. Model numbering is that of the original MMC pool. **C,D** Ribbon representations of the models selected by NNLS without (**C**) or with (**D**) error weighting. The models were all superimposed using the N-terminal 63-270 domain, and they were grouped into four (**C**) or three (**D**) classes starting from their respective  $P(r)$  shapes as plotted in **A** and **B**, also considering the  $R_g$  values, shown together with the models' percent contribution.

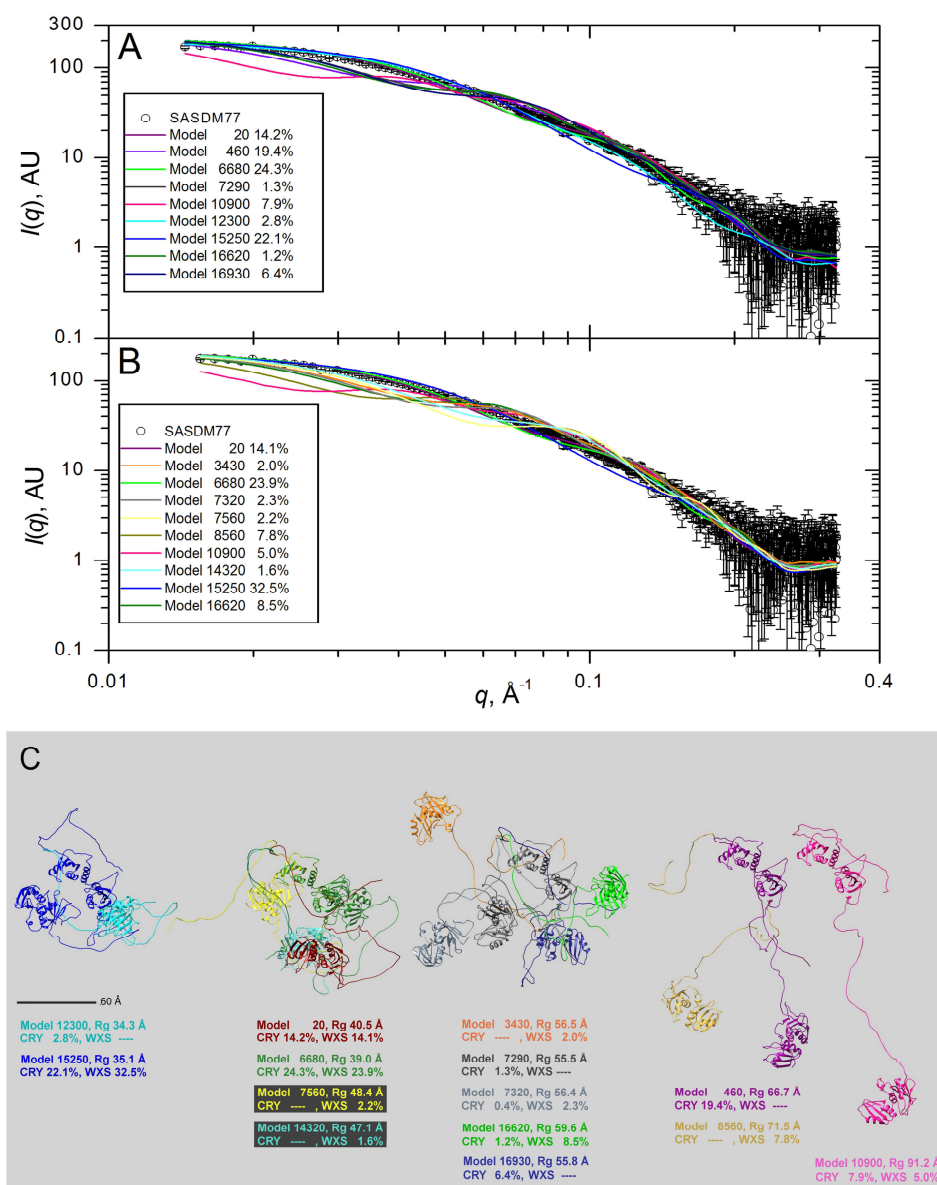


**Figure S6** A,B  $I(q)$  vs.  $q$  of the individual MMC-generated Q9UKA9 models selected by NNLS from the CRY SOL 2.8-produced set (A), and from the WAXSiS-produced set comprising only the models selected by both the two  $P(r)$  and the  $I(q)$  CRY SOL 2.8 NNLS fits (B), with their percent contribution (various colours, see inside panels), superimposed to the SASDM77 experimental data. Model numbering is that of the original MMC pool. C,D Ribbon representations of the models selected by NNLS in panels A and B, respectively. The models were all superimposed using the N-terminal 63-270 domain, and they were grouped using the  $P(r)$ -derived clustering of Figure S3C, with the removal of the leftmost class and the insertion of a single very extended model. Together with their percent contribution in each NNLS fit (CRY, CRY SOL; WXS, WAXSiS), the  $R_g$  of each model is also reported.